Supporting Information

A synergistic optical strategy for enhanced deep-tumor penetration and therapy in the second near-infrared window

Di Wu,[†abc] Xiaohong Chen,[†a] Jiajing Zhou,[c] Yuxuan Chen,[a] Tao Wan,[a] Yi Wang,[a] Aifu Lin,[d] Yeping Ruan,[e] Zhong Chen,[a] Xiangrong Song,[f] Wenjun Fang,*[b] Hongwei Duan,*[c] and Yuan Ping*[a]

[a] College of Pharmaceutical Sciences, Zhejiang University, Hangzhou 310058, China.

[b] Department of Chemistry, Zhejiang University, Hangzhou 310028, China.

[c] School of Chemical and Biomedical Engineering, Nanyang Technological University, Singapore 637457, Singapore.

[d] College of Life Sciences, Zhejiang University, Hangzhou 310058, China.

[e] College of Pharmaceutical Sciences, Zhejiang Chinese Medical University, Hangzhou 310053, China.

[f] Department of Critical Care Medicine, State Key Laboratory of Biotherapy, West China Hospital, Sichuan University, Chengdu, China

[†] D. Wu and X. Chen contributed equally to this work.

*Corresponding author: pingy@zju.edu.cn; hduan@ntu.edu.sg; fwjun@zju.edu.cn

Experimental Section

Chemicals and materials. Hydrogen tetrachloroaurate (III) trihydrate ($HAuCl_4 \cdot 3H_2O$) was purchased from Alfa Aesar. 1, 3, 5-trimethylbenzene was purchased from Tokyo Chemical Industry Co., Ltd. Dopamine hydrochloride, Pluronic F127 block copolymer (F127), hydroxylamine hydrochloride, silver nitrate, hydroquinone, hexadecyl trimethyl ammonium bromide (CTAB), sodium brohydride, 4-(2-hydroxyethyl)-1-piperazineethanesulfonic acid (HEPES) were purchased from Sigma-Aldrich. Fetal bovine serum (FBS), McCoy's 5A medium, Dulbecco's Modified Eagle's Medium (DMEM), Texas Red™-X (Succinimidyl Ester), propidium iodide, LIVE/DEAD viability/cytotoxicity kit, and the Pierce™ Protease Activity Assay Kit (PAAK) was purchased from Thermo Fisher Scientific, United States. The cell counting kit-8 (CCK-8) was purchased from DOJINDO, Japan. Anti-collagen I antibody, goat anti-rabbit IgG H&L (Alexa Fluor® 488), anti-caspase-3 antibody and donkey polyclonal secondary antibody to rabbit IgG-H&L (Alexa Fluor® 488) were purchased from Abcam Inc. (China). Fresh chicken breast tissue was purchased from WalMart. Ultrapure water (18.2 MΩ·cm) was purified using a Sartorious AG arium system and used in all experiments. All other chemicals and bioreagents were purchased from Sigma Aldrich unless otherwise declared.

Synthesis of AuNR. Au nanorods were synthesized using a seed-mediated growth method. Briefly, the gold seeds were prepared by adding 5 mL of $HAuCl_4$ (0.5 mM) to 5 mL of CTAB solution (0.2 M). Then, 600 μL of freshly prepared $NaBH_4$ (10 mM) was quickly added to the mixture with vigorous stirring for 60 s. After incubated at 30 °C for 1 h, the mixture was used as seed solution for further synthesis. Afterwards, a growth solution was prepared by adding 60 μL of $AgNO_3$ (0.1 M) to a mixture of 5 mL of $HAuCl_4$ (1 mM) and 5 mL of CTAB (0.2 M), followed by adding 300 μL of hydroquinone (0.1 M). Finally, seed solution was added to the solution to initiate the growth of AuNR. The solution was incubated at 30 °C overnight and AuNR was collected by centrifugation.

Synthesis of AuNR@mPDA. Mesoporous polydopamine coated gold nanorods were prepared in a seed-mediated growth method. Briefly, 50 mg of F127 were dissolved in 1.5 mL of ethanol and further mixed with 1.5 mL of AuNR solution, 20 μL of 1, 3, 5-trimethylbenzene (TMB), 15 mg of dopamine hydrochloride. After

sonication for 3 min, 90 μL of $NH_3 \cdot H_2O$ were added subsequently to trigger the polydopamine self-polymerization. The raw products were separated by centrifugation. Ethanol and ultrapure water were used to remove TMB and F127. The similar coating could be performed by replacing AuNR with gold nanoparticles, silicon dioxide nanoparticles and magnetic nanoparticles. Then PEGylation of AuNR@mPDA was conducted in 10 mM bicine buffer (pH = 8.5) by adding thiol polyethylene glycol (PEG-SH, MW: 5,000 Da). Unreacted PEG-SH could be removed by centrifugation. All AuNR@mPDA nanoparticles for in vitro and in vivo tests were PEGylated prior to use and will only be noted as AuNR@mPDA for clarity unless otherwise stated.

Enzyme-dye bioconjugation. Texas Red™-X, succinimidyl ester was used to label the protein according the manufacturer instruction with some modifications. Briefly, 10 mg/mL of proteins was mixed with 200 μg/mL of Texas Red in 10 mM bicine buffer (pH = 8.5) at room temperature with continuous stirring. After 90 min reaction, 1.5 M of freshly prepared hydroxylamine (pH = 8.5) was used to stop the reaction and the unreacted dye was then removed by dialysis (MWCO: 10, 000 Da) against 1 × PBS (pH = 7.4) for 48 h. The protein-dye conjugates could be stored at 4 ℃ for further use. The bioconjugation was confirmed by recording the spectrum with a UV-Vis spectrometer and a fluorometer.

Enzymatic activity assay. The Pierce™ protease activity assay kit (Thermo Fisher) was used to demonstrate the enzymatic activity of each sample following the kit instruction. Succinylated casein that is used in the assay method is native casein treated with succinic anhydride to block primary amines on the protein surface. In the presence of active enzyme, the succinylated casein is cleaved at peptides bonds, leading to exposure of blocked primary amines that further react with trinitrobenzenesulfonic acid. The orange-yellow products are measured by microplate reader at 450 nm, and the absorbance is directly proportional to enzymatic hydrolysis of the test enzyme. According to the instructions, the concentration-dependent assays of papain, Texas Red-labeled Pap and trypsin were first carried on to confirm the protease activity of as-prepared proteins, while the trypsin serves as a general standard for comparison of overall activity among different samples. In addition, 100 μg/mL of Pap and modified Pap of peptide digestion at 4, 25, 30, 40, 50, 60, 70 °C for 20 min was performed to evaluate the temperature effect on the enzymatic activity. The enzyme test of each condition was repeated three times.

Enzyme loading and release. To determine the loading capacity, 1000 μg/mL of Texas Red was mixing with 300, 600, 1000 μg/mL Texas Red-labeled papain in a neutral buffer (PBS, 10 mM, pH = 7.4). After loading for a set time (20, 40, 60, 120, 180, 240 min), the AuNR@mPDA-Pap complex centrifuged down and re-suspended in fresh buffer for further use. Meanwhile, the fluorescence intensity of the supernatant (*Fs*) can be determined on a Horiba fluorometer, and was compared with fluorescent intensity of enzyme solution (*F0*) at a determined concentration (*C0*). The enzyme loading capacity (σ) was calculated by the following equation (1):

$$\sigma = \frac{(F0 - Fs) \times C0}{Fs} \quad (1)$$

where *C0* was the concentration of enzyme solution.

The sequential enzyme release profiles in neutral buffer (pH = 7.4), acidic buffer, NIR-II irradiation (0.3 W/cm^2, 1.0 W/cm^2) were recorded as follows. Firstly, 10 mL of AuNR@mPDA-Pap complex (1 mg/mL) was prepared in neutral buffer (10 mM PBS, pH = 7.4, 150 mM ionic strength) and acidic buffer (10 mM PBS, pH = 6.0, 150 mM ionic strength). Then, 2 mL of the solution was withdrawn and the release data was collected using the fluorometer. For NIR-II irradiation study, 10 mL of AuNR@mPDA-Pap solution (1 mg/mL) prepared in acidic solution was used the mimic the tumor extracellular environment. The irradiation was immediately conducted at a power density of 0.3 W/cm^2 and 1.0 W/cm^2. And 2 mL of the solution was withdrawn and the release data was collected using the fluorometer at pre-determined time intervals (30 min).

Photothermal conversion test. Photothermal conversion tests were carried on with 400 μL of mPDA, AuNR, AuNR@mPDA, AuNR@mPDA-Pap (200 μg/mL) at pre-determined concentration under NIR-II irradiation (1064 nm, 1.0 W/cm^2) in 1.5 mL tube. Fresh chicken breast tissues at different thickness were placed on the top of tubes for deep penetration simulation. The temperature change of the solution was recorded by an IR camera every 30 s. To obtain the photothermal conversion efficiency (η), AuNR@mPDA-Pap solution ($OD_{1064\,nm} = 1$) suspended in a quartz cuvette was exposed to an NIR laser for 20 min and the temperature was recorded in the heating and natural cooling stage. The efficiency η was calculated according to the equation reported before as follows:

$$\eta = \frac{hS(T_{max} - T_{surr}) - hS(T_{max.water} - T_{surr})}{P(1 - 10^{-A_{1064}})} \quad (2)$$

where h is the heat transfer coefficient, S is the surface area of sample container; T_{max}, T_{surr} and $T_{max.water}$ are the highest temperature the sample reached, the ambient room temperature, and the highest temperature the water reached respectively; P is the laser power density and A_{1064} is the LSPR absorbance of AuNR@mPDA-Pap at 1064 nm. The value of hS in the equation above is calculated by Eq. (3)

$$hS = \frac{mc + m'c'}{\tau} \quad (3)$$

where m, m', c and c' are the mass of AuNR@mPDA-Pap solution and the quartz cuvette, the heat capacity of AuNR@mPDA-Pap solution and the quartz cuvette, respectively; The value of τ is the characteristic thermal time constant which can be determined from the curve of sample cooling time *versus* negative natural logarithm of the temperature driving force ($\frac{\Delta T}{\Delta T_{max}}$).

Circular dichroism analysis. The freshly prepared enzyme solution and the enzyme collected from the supernatant in release study were kept at a concentration of 0.2 mg/mL and were used to validate the reversible loading. A far ultra-violet circular dichroism analysis was conducted on a JASCO J-1500-150 ST spectrometer at room temperature (Spectral range: 200 - 260 nm; Scanning rate: 50 nm/min). The band width, response time and data pitch were set as 1 nm, 1 s and 0.2 nm, respectively. Three individual scans were accumulated per spectrum and raw data were processed using JASCO software package.

Cell culture and cytotoxicity assay. HT-29 human colon cancer cells and 3T3 fibroblast cells were cultured in McCoy's 5A medium and DMEM, respectively, supplemented with 10% FBS and 1% antibiotics at 37 °C under 5% CO_2 atmosphere. The cells were treated with 0.25% trypsin and collected when 80% of the flask was confluent. CCK-8 was used to assess cytotoxicity of each treatment mentioned in the paper. Briefly, 100 μL of HT-29 or 3T3 cells in the log phase of growth were seeded in a 96-well plate with a cell density of 1.0×10^4 cells/well. After overnight incubation, the cells were treated with AuNR@mPDA-Pap at specific concentrations (0, 100, 200, 400, 600, 800, 1000 μg/mL) and incubated for 24 h. For deep penetration study, the fresh chicken breast tissues at different thickness were placed on the top of cell culture

plates, and further photothermal therapy (1064 nm, 1.0 W/cm^2) on two cell lines were performed in an incubator of 37 °C. After the specific treatment, 10 μL of CCK-8 solution were added into each well and incubated for another 4 h. In this test, the amount of the formazan dye, generated by the activities of dehydrogenases in cells by reduction of WST-8, is directly proportional to the number of living cells. Thus, absorbance of each test solution measured by a microplate reader at 450 nm was used to determine the cell viability. Each treatment was conducted with three repeating tests. For hemolysis analysis, blood cells were obtained from the mice and incubated with different concentrations of Au@mPDA-Pap for 4 h. The PBS and deionized water were used as negative and positive controls, respectively. The samples were then centrifuged, and the supernatant were used for absorbance measurement.

Enzymatic activity assay of gelatin digestion unit. The enzymatic activity of enzyme-loaded nanoparticles is evaluated by the assay of gelatin digestion and is expressed as gelatin digestion unit (GDU) according to previous report with some modifications. In a typical test, 2.5 mL of gelatin solutions (1% wt. in 10 mM PBS buffer) in a 4 mL vial was mixed thoroughly with 50 μL of AuNR@mPDA (200 μg/mL), AuNR@mPDA-Pap (200 μg/mL) with one more repetitive test, respectively. The mixture solution was irradiated with a 1064 nm NIR laser at a power density of 0.3 W/cm^2 for 20 min and then the reaction was quenched by adding 100 μL of H_2O_2 (3%). Further, pH of the solution was adjusted to 6.0 with NaOH and 200 μL of formaldehyde (37%) was added with constant stirring. Titration test was performed with 0.05 N NaOH until the pH reached 8.0. The titration volume (V) of NaOH was recorded in each test, and the GDU was calculated by Eq. (4) as follows:

$$\text{GDU} = (V_{\text{test}} - V_{\text{blank}}) \times \text{N} \times 14\ \text{mg} \times 1000/\text{mg enzyme} \quad (4)$$

where V_{test} and V_{blank} are the titration volume of NaOH in the sample test, and blank test, respectively; N is normality of NaOH; 14 mg is the weight of one millimole nitrogen.

3D tumor spheroid culture and penetration test. The 3D tumor spheroid was constructed according the previous method with modifications. Briefly, 60 μL of hot agarose solution (2 %) was added quickly into a sterile 96-well plate and naturally cooled at room temperature for solidification. The solid gel was washed by sterile 1 × PBS buffer three times and then sterilized under UV light for three hours. The gel plate could be sealed and kept at 4 °C for further use. Then, 200 μL of HT-29 cell suspension

in McCoy's 5A medium was seeded onto the agarose gel at a density of 10, 000 cells per well, and were cultured at 37 °C with 5 % CO_2 for five days to form the 3D tumor spheroid. The cultured 3D tumor spheroid was washed by PBS buffer and then used to evaluate the penetration of enzyme-loaded nanohybrids. Prior to the test, the nanohybrids were labeled with Texas Red for fluorescence tracking. After incubated with 10 μg/mL AuNR@mPDA-Pap for one hour, the spheroids were irradiated under intermittent NIR irradiation (0.3 W/cm^2) for 15 min every one hour for three times. Solution temperature changes were observed by IR camera and were kept at 42 °C *ca*. to avoid hyperthermal ablation. Then the tumor spheroids were fixed with 4% paraformaldehyde, and carefully transferred to confocal dishes. Penetration tests were performed using Z-Stack mode by an LSM810 confocal laser scanning microscope (Carl Zeiss, Germany). Image analysis of the fluorescence was performed by using ImageJ. Diffusion profiles of relative fluorescence intensity (*C*) and the diffusion distance (*r*) for the nanoparticles were fitted to the following diffusion Eq. (5) to obtain the diffusion coefficient (*D*) in the 3D tumor spheroid:

$$C(r,t) = A \times erfc\left(\frac{r}{\sqrt{2tD}}\right) + B \quad (5)$$

where erfc is the complementary error function; *t* is the diffusion time; A and B are the constant for the function. The nonlinear curve fitting was performed by using fminsearch in MATLAB R2019a.

Ex vivo photothermal activation of stromal depletion. All procedures including ex vivo and in vivo tests were carried out in compliance with College of Pharmaceutical Sciences of Zhejiang University and followed the Regulation on the Administration of Laboratory Animals (2017 Revision) established by the State Council, the People's Republic of China. The xenografted tumors of HT-29 cell lines were established by subcutaneous injection of 2 × 10^6 cancer cells suspended in 200 μL of normal saline in nude mice (National Cancer Institute Animal Production Facility) for further use. The solutions of saline (200 μL), AuNR@mPDA (200 μg/mL, 200 μL) or AuNR@mPDA-Pap (200 μg/mL, 200 μL) were then peritumorally injected into HT-29 tumor-bearing mice when the volume of tumor reached 60 mm^3. After 24 h, the tumors were exposed to intermittent 1064 nm irradiation at a power density of 0.3 W/cm^2 for 15 min every one hour for three repetitive times (the tumor temperature was controlled to be 42 ºC *ca*. under observation of infrared thermal camera). The treated mice were euthanized

and tumors were extracted, washed with saline and fixed in 4% paraformaldehyde for overnight. Then immunofluorescent staining of the tumors was performed to investigate the collagen type I digestion. The tumor sections were washed three times with PBS for 5 min, followed by incubation with 15% sucrose solution overnight. Again, the sections were incubated with 30% sucrose solution overnight at 4 ºC. After adding optimum cutting temperature compound (OCT), the sections were cured under liquid nitrogen, and stored at -80 ℃ for further analysis. Further mounting of specimen onto the holder, freezing, attachment of the holder to the pre-cooled cryo-microtome and sectioning were performed. The frozen sections were treated as thin as 2 μm, and the sections were fixed in acetone for 10 min at -20 ℃. The next day samples were incubated with 3% BSA in PBS solution at room temperature for 1 h, following by washing with PBS. The sections were then incubated with anti-collagen I antibody solution (1:500 in PBS) at 4 ºC for 12 h. After being washed with PBS to remove excessive antibody, the sections were counterstained with Alexa Fluor 488 conjugated goat anti-rabbit IgG H&L (1:1000 in PBS) at room temperature for 1 h. The cell nucleus was stained with DAPI (1:1000 in PBS). The stained sections were then observed under an LSM 710 confocal laser scanning microscope.

In vivo fluorescence imaging. The tumor-bearing nude mice were first treated with saline (200 μL), AuNR@mPDA (200 μg/mL, 200 μL), and AuNR@mPDA-Pap (200 μg/mL, 200 μL). After photothermal activation of enzyme by preNIR irradiation, the representative fluorescence images of mice in vivo were captured after 24 h of injection using a Lumina IV animal imager. Then, the mice were immediately euthanized and the major organs (heart, liver, spleen, lung, and kidney) were extracted. The organs were washed three times by PBS and fluorescence images of organs were captured.

Pharmacokinetics of AuNR@mPDA. To evaluate the blood circulation, the AuNR@mPDA-Pap nanoparticles (200 μL, 200 μg/mL) were administrated into the tumor-bearing mice (n = 3) intravenously. After a certain time of injection, the blood samples were harvested from eyes, and were then treated by aqua regia (dangerous) for digestion. The acidic mixtures were then carefully neutralized by ammonia. The supernatant was collected by centrifugation and purified by a 220 nm cut-off filter. Further quantitative analysis of Au was performed by using inductively coupled plasm

mass spectrometry (ICP-MS). The amount of AuNR@mPDA-Pap was normalized to the percentage of injected dose per gram of blood (%ID/g).

In vivo photothermal therapy on mice model. We performed comparative experiments with HT-29 tumor-bearing mice treated with saline, AuNR@mPDA, and AuNR@mPDA-Pap solutions with or without preNIR-induced stromal depletion for specificity. The mice were systematically administered with saline (200 μL), AuNR@mPDA (200 μL, 200 μg/mL) and AuNR@mPDA-Pap (200 μL, 200 μg/mL) via intravenous injection. After 24 h, the tumors were exposed to 1064 nm irradiation (0.3 W/cm^2) for 15 min every one hour for three repetitive times, with the tumor temperature at 42 °C *ca*. to minimize the hyperthermal damage. After one day of the pre-treatment, tumors of living mice were treated with NIR-II irradiation (1.0 W/cm^2) for 5 min. During the laser irradiation, an infrared thermal camera was used to monitor the temperature of the mouse skin. For the buried tumor therapy model, a piece of 5 mm-thick chicken breast tissue was placed on the top of the tumor site. The temperature of the tumor site underneath the chicken breast tissue was monitored by a type of K/J thermocouple dual input thermometer. After the therapy, the tumor sizes were measured with a caliper, and the mice weight was recorded every other day for two weeks. Calculation of the tumor volume (V) was performed using the following equation: Tumor volume = [Length × Width^2]/2. The relative tumor volume was determined as V/V_0 (V_0 is the tumor volume on the day of injection). The blood samples were prepared after 24 h of the therapy and the serum was obtained by centrifugation at 4, 000 rpm for 10 min. Hematological parameters including total protein, albumin, globulin, total bilirubin, ALT, AST, BUN and uric acid were investigated.

Immunofluorescence and histopathology. After 14 days of the therapy, the extracted tumors were thawed and fixed in 4% paraformaldehyde overnight at room temperature. The sections were washed three times in PBS for 5 min, followed by incubation with 15% sucrose solution overnight at room temperature. Again, the sections were incubated with 30% sucrose solution overnight at 4 ºC. Then optimum cutting temperature compound was added, after curing under liquid nitrogen, and then the sections were stored at -80 ℃ for further analysis. Mounting of specimen onto the holder, freezing, attachment of the holder to the pre-cooled cryomicrotome, sectioning, the frozen sections can be as thin as 2 μm, and the sections were fixed in acetone for 10 min at -20 ºC. After the frozen section, the sections were stained with

immunofluorescence staining and hematoxylin-eosin (H&E). The immunofluorescence staining was performed as following procedure that the sections were dried at room temperature for 1.5 h and then washed by PBS containing 0.1% Triton X-100 three times. Then the samples were incubated with 3% BSA in PBS solution at room temperature for 1 h, following by washing with PBS to remove BSA. Follow incubated with anti-caspase-3 antibody solution (1:500 in PBS) at 4 ºC for overnight. After being washed with PBS to remove excessvie antibody, the sections were counterstained with Alexa Fluor 488 conjugated goat anti-rabbit IgG H&L (1:1000 in PBS) at room temperature for 3 h. The cell nucleus was stained with DAPI (1:1000 in PBS). The stained sections were then observed under a confocal laser scanning microscope. Histopathology procedure for sequential was conducted as follows: The frozen sections were thawed, and the sections were fixed in 4% buffered formaldehyde (30 min) followed by sterile water washing three times, and then were incubated with hematoxylin for 2 min. The sections were washed three times in sterile water and incubated with 1% hydrochloric acid for 30 s and 1% ammonia 10 s, respectively. After washing three times, the sections were dehydrated in different concentrations of ethanol. Then, the sections were placed in tissue transparent solution, ensuring transparency slice, which slice facilitate observation and preservation, retrieval of sections to room temperature mounting, observation.

Characterization. Transmission electron microscopy (TEM) observations were conducted on a JEOL electron microscope (JEM 2010) at an acceleration voltage of 300 kV. Scanning electron microscopy (SEM) images were obtained on an FESEM (JSM-6700F, Japan). EDX spectra and STEM images were obtained on a 200 kV JEM 2100F transmission electron microscope (JEOL, Japan) equipped with an EDX and stem detector. UV-Vis-NIR (400 nm - 1400 nm) spectra were recorded on a Cary5000 spectrometer and fluorescence measurements were recorded on a Horiba fluorometer by exciting the samples at 580 nm and recording the emission data at 610 nm. Size distribution and zeta potentials were measured using a Malvern Dynamic Light Scattering (Nano ZS). The average size results recorded in this study only represented the change of the size of AuNRs with surface coating, which could not characterize the hydrodynamic size of anisotropic nanorods. Sample temperature was recorded on an FLIR T420 camera. Cell observations were conducted on an Olympus IX71 inverted

microscope, a Photometrics CoolSNAP-cf cooled CCD camera and a PIXIS: 100B spectroscopy CCD.

Statistical analysis. The tumor volume data in this paper were analyzed by Graphpad prism 8.0. The statistical significance was analyzed using two-way analysis of variance (ANOVA) with a Dunnett post hoc test. The p-value less than 0.05 was considered significant (*$P < 0.05$, **$P < 0.01$, ***$P < 0.001$, ****$P < 0.0001$).

Results and Discussion

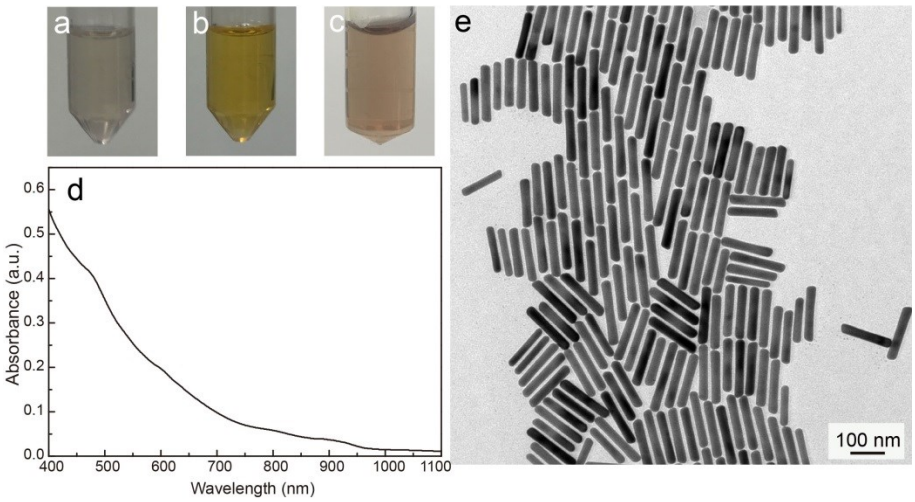

Fig. S1 Photographs of the solution of (a) gold nanoseeds, (b) gold precursers, and (c) gold nanorods. (d) UV-Vis-NIR spectrum of gold nanoseeds for nanorods synthesis. (e) High length-width ratio gold nanorods.

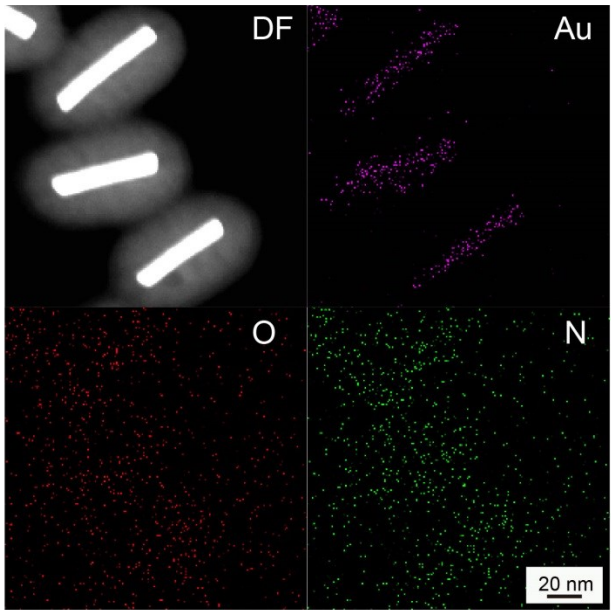

Fig. S2 DF-STEM image and EDX elemental mapping of AuNR@mPDA.

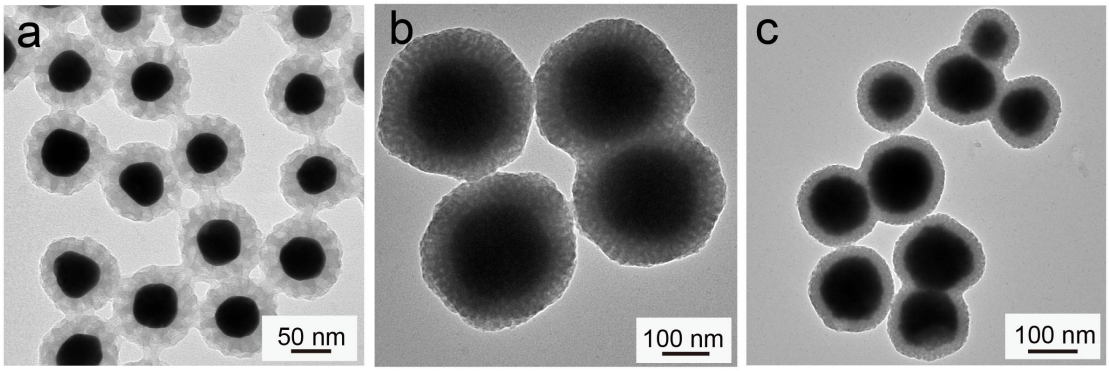

Fig. S3 TEM images of mesoporous polydopamine coated (a) Au nanoparticles, (b) SiO_2 nanoparticles, and (c) magnetic nanoparticles.

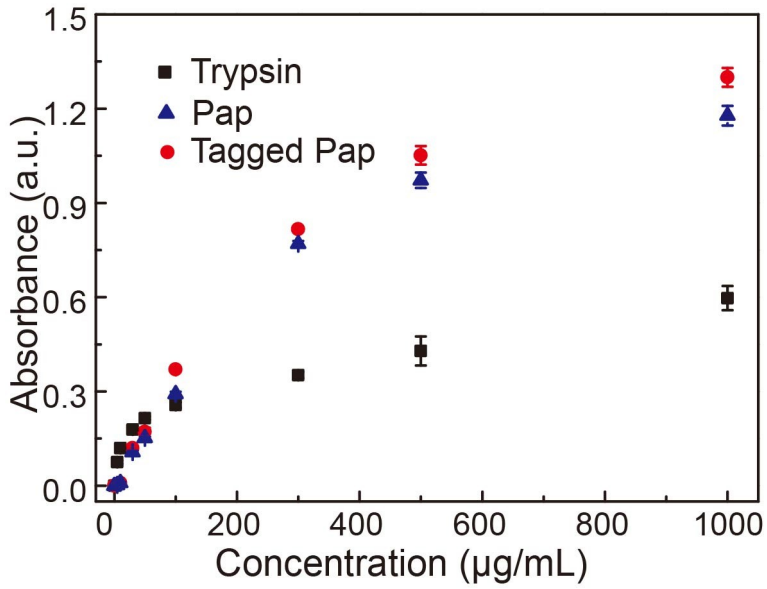

Fig. S4 Protease activity of trypsin, Pap, and tagged Pap at varing concentrations (10, 20, 50, 100, 300, 500, 1000 μg/mL) evaluated by protease activity assay kit using a UV-Vis spectrometer (n = 3).

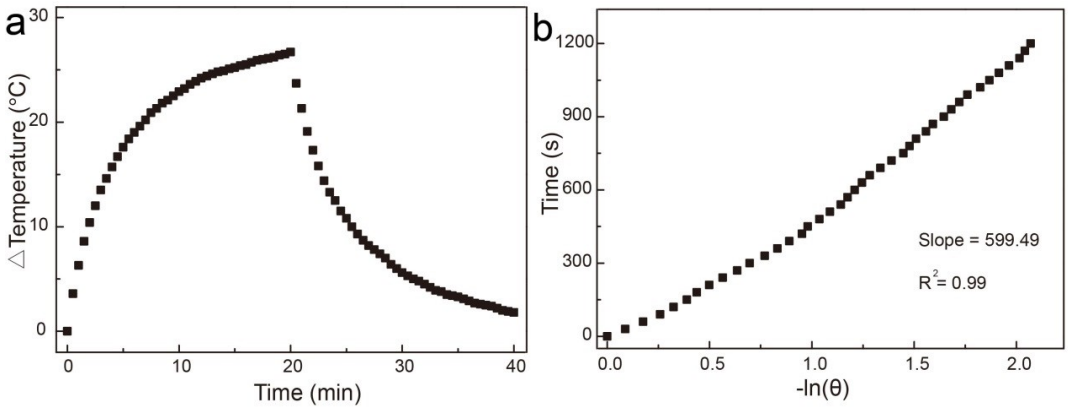

Fig. S5 (a) Plot of temperature of AuNR@mPDA-Pap solution ($OD_{1064\ nm}$ = 1.0) under photothermal heating and natural cooling process in a quartz cuvette in 40 min. (b) Plot of time *versus* negative natural logarithm of the temperature driving force ($\triangle T/\triangle T$max) in the natural cooling process.

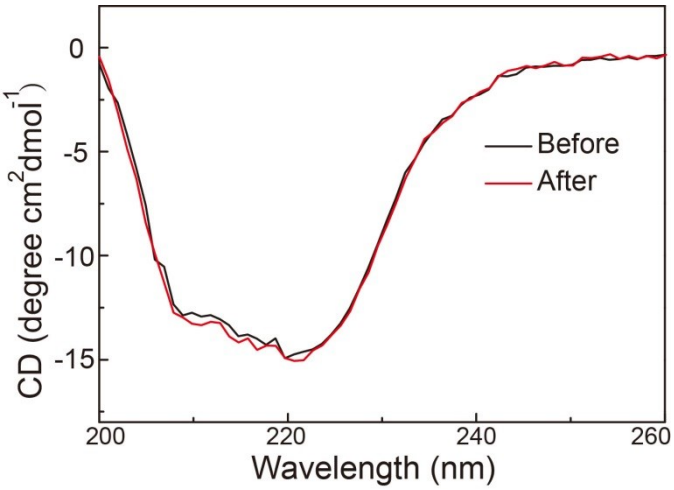

Fig. S6 Circular dichroism analysis of the enzyme (0.2 mg/mL) before the loading and released from AuNR@mPDA-Pap.

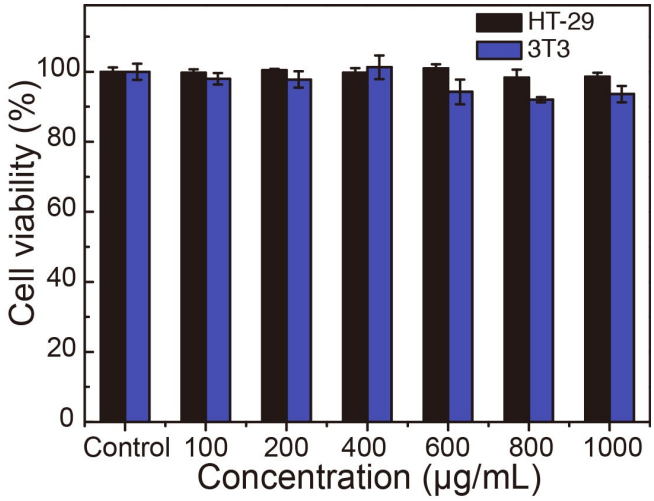

Fig. S7 Cell viability (CCK-8) of HT-29 and 3T3 cancer cells after the treatment of AuNR@mPDA-Pap at varing concentrations (100, 200, 400, 600, 800, 1000 μg/mL). The error bars represent standard deviations (n = 3).

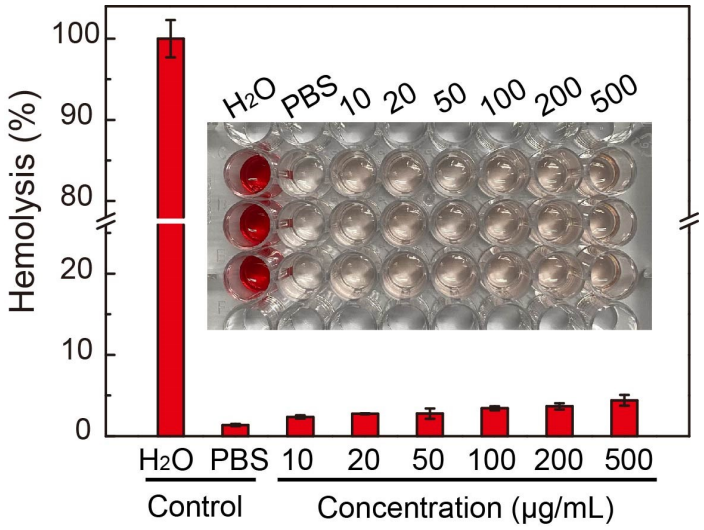

Fig. S8 Hemolysis of PEGylated AuNR@mPDA-Pap nanoparticles after incubation with red blood cells with various concentrations, PBS as a negative and deionized water as a positive control, respectively. Inset: hemolysis photographs of the solution supernatant after centrifugation. The error bars represent standard deviations (n = 3).

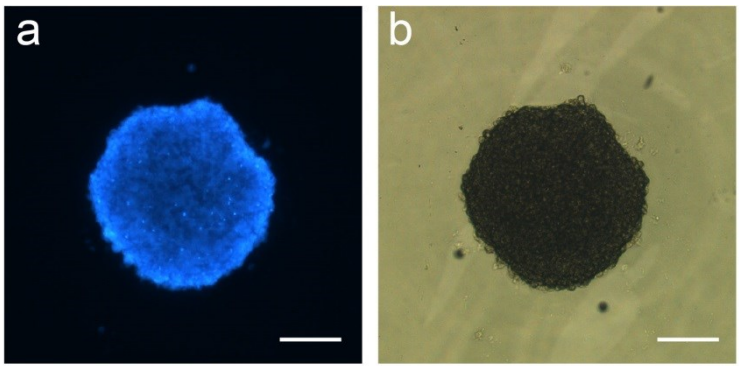

Fig. S9 (a) Fluorescence and (b) bright-field image of a 3D HT-29 tumor spheroid cultured on agar gel (scale bar: 200 μm). Cell nucleus was stained with DAPI for fluorescent observation.

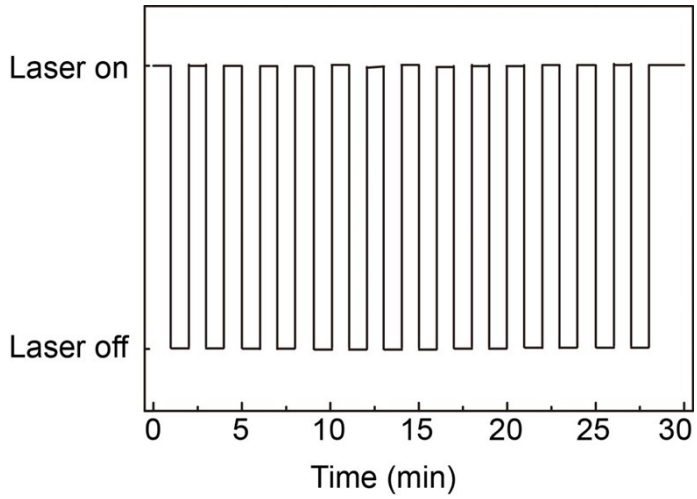

Fig. S10 On-off state of the laser (1064 nm, 0.3 W/cm^2) as an intermittent mode for photothermal activation under the control of infrared thermal camera. The tumor temperature was kept at 42 °C *ca.*.

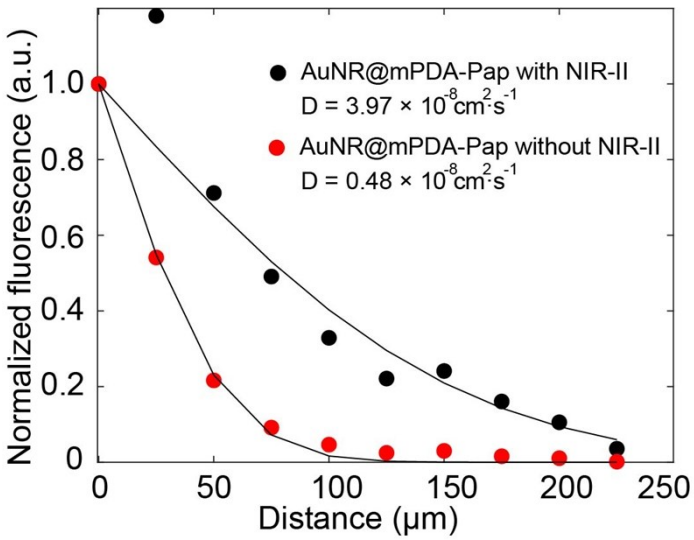

Fig. S11 Normalized fluorescence of AuNR@mPDA-Pap with diffusion distance in 3D tumor spheroids. The image fluorescence was analyzed by using ImageJ. The diffusion coefficients (D) of AuNR@mPDA-Pap with or without NIR-II irradiation were obtained by fitting the resulting profiles to a drug diffusion model via fminsearch in MATLAB.

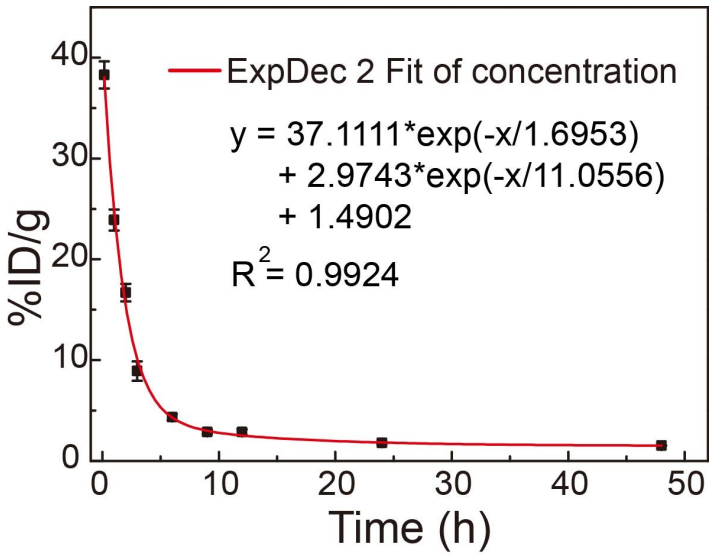

Fig. S12 Blood circulation profiles of AuNR@mPDA-Pap in tumor-bearing mice (n = 3). The blood concentration of nanoparticles (Au) at different time points was confirmed by ICP-MS.

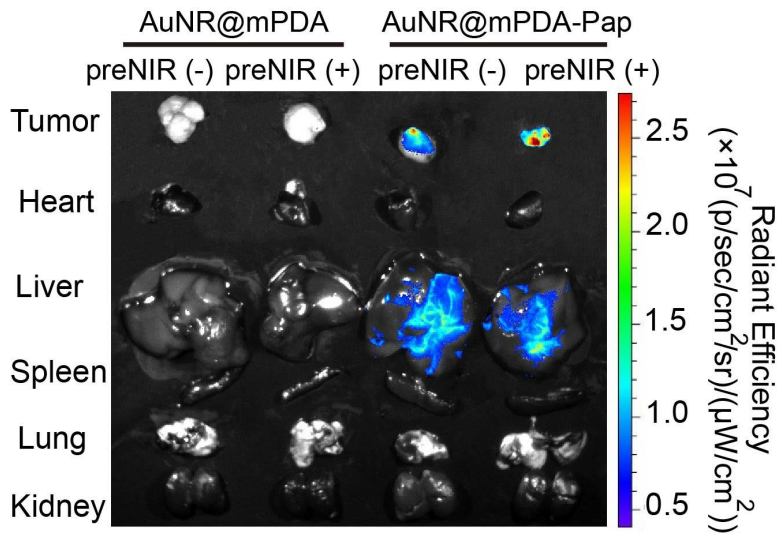

Fig. S13 Fluorescence imaging of tumors and major organs from HT-29 tumor-bearing mice at 24 h after systemic administration of saline, AuNR@mPDA, and AuNR@mPDA-Pap (200 μg/mL) with or without preNIR irradiation for stromal depletion.

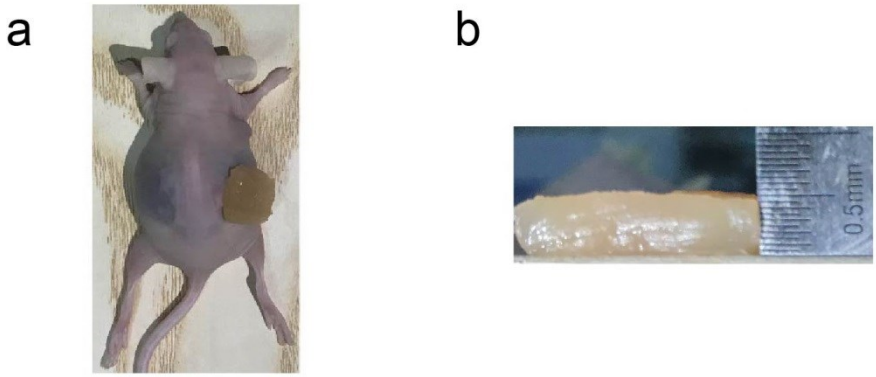

Fig. S14 Photographs of (a) a two tumors-bearing mouse covered with (b) a piece of 5 mm-thick chicken breast tissue.

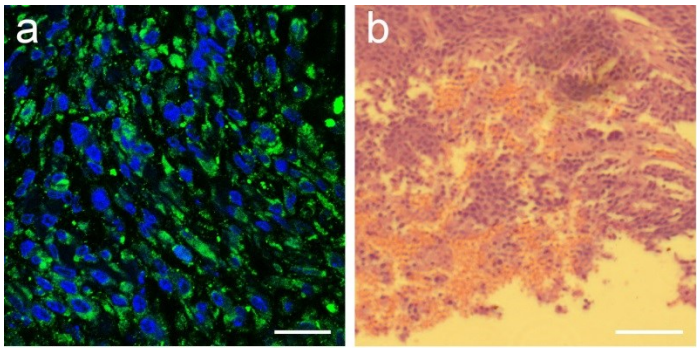

Fig. S15 (a) Immunofluorescence staining and (b) histological H&E staining of tumor tissue in the group of mice after the therapy covered by 5 mm-thick chicken breast tissue (scale bar: (a) 50 μm; (b) 100 μm).

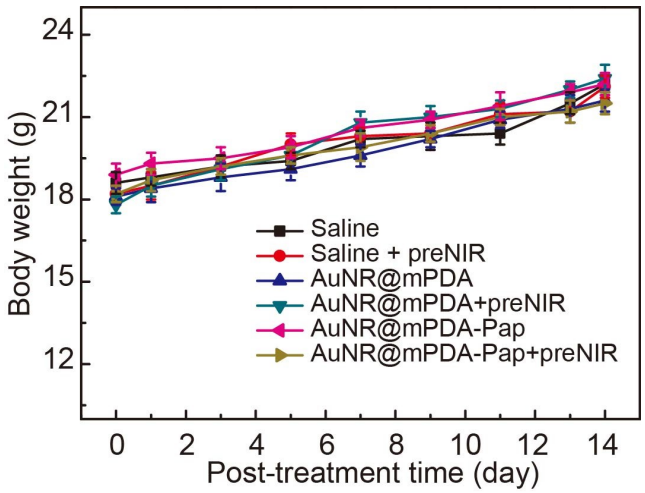

Fig. S16 Bodyweight changes of tumor-bearing mice in different groups recorded in 14 days after the photothermal therapy (n = 4).

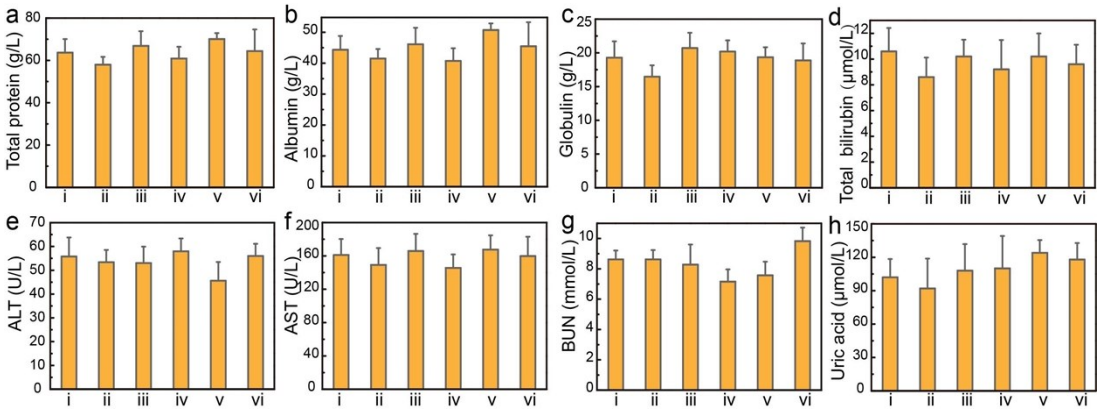

Fig. S17 Blood chemistry analysis of tumor-bearing mice 14 days after the different treatment including (a) total protein, (b) albumin, (c) globulin, (d) total bilirubin, (e) ALT, (f) AST, (g) BUN, and (h) uric acid. Group i, ii, iii, iv, v, and vi represent the group of saline, saline with preNIR, AuNR@mPDA, AuNR@mPDA with preNIR, AuNR@mPDA-Pap, and AuNR@mPDA-Pap with preNIR respectively. All six groups were post-treated with NIR irradiation for photothermal therapy. (n = 4).

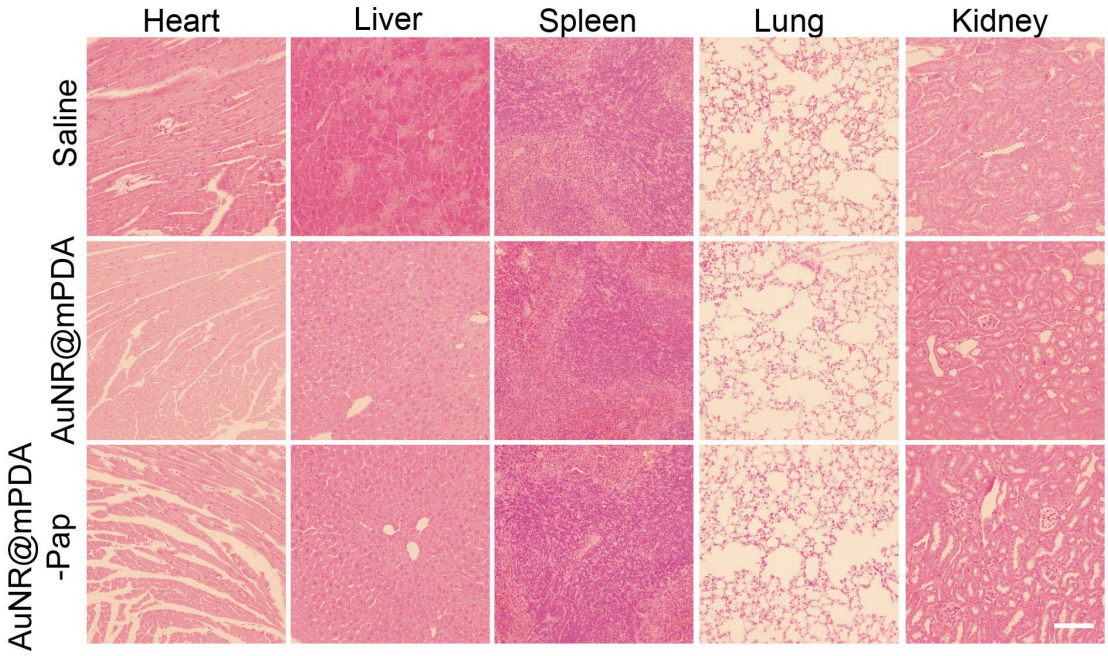

Fig. S18 Histological analysis of major organs (heart, liver, spleen, lung and kidney) from the mice treated with saline, AuNR@mPDA, AuNR@mPDA-Pap stained with hematoxylin and eosin (scale bar: 100 μm).